Intermolecular hydrogen-bonded organic semiconductors—Quinacridone versus pentacene

Eric Daniel Głowacki,[1,a)] Lucia Leonat,[2] Mihai Irimia-Vladu,[1,3] Reinhard Schwödiauer,[3] Mujeeb Ullah,[4] Helmut Sitter,[4] Siegfried Bauer,[3] and Niyazi Serdar Sariciftci[1]
[1]*Linz Institute for Organic Solar Cells (LIOS), Physical Chemistry, Johannes Kepler University Linz, Austria*
[2]*Faculty of Applied Chemistry and Materials Science, Politehnica University of Bucharest, Bucharest, Romania and National Institute for Electrical Engineering, IPCE-CA, Bucharest, Romania*
[3]*Soft Matter Physics, Johannes Kepler University Linz, Austria*
[4]*Institute of Solid State Physics, Johannes Kepler University Linz, Austria*

(Received 13 February 2012; accepted 23 June 2012; published online 12 July 2012)

Quinacridone is a five-ring hydrogen-bonded molecule analogous in structure and size to the well-known organic semiconductor pentacene. Unlike pentacene, quinacridone has limited intramolecular π-conjugation and becomes highly colored in the solid state due to strong intermolecular electronic coupling. We found that quinacridone shows a field-effect mobility of 0.1 $cm^2/V{\cdot}s$, comparable to mobilities of pentacene in similarly prepared devices. Photoinduced charge generation in single-layer quinacridone metal-insulator-metal diodes is more than a hundred times more efficient than in pentacene devices. Photoinduced charge transfer from quinacridone to C_{60} is not effective, as evidenced by measurements in heterojunctions with C_{60}. Hydrogen-bonded organic solids may provide new avenues for organic semiconductor design. © *2012 American Institute of Physics*. [http://dx.doi.org/10.1063/1.4736579]

Organic semiconductors differ in many respects from inorganic ones. Small molecular organic semiconductors and polymers form van der Waals solids, where the relatively weak intermolecular interactions results in materials with low dielectric constant (ε_r). Inefficient electric field screening and disorder in organic semiconductors lead to high exciton binding energy, as well as to localization effects and hopping transport.[1]

Molecules where intramolecular π-conjugation is interrupted by functional groups such as carbonyl and secondary amines are typically not considered for organic semiconductor applications.[2,3] Recent work on hydrogen-bonded indigoids[4,5] has shown that these small and 'poorly' conjugated molecules show ambipolar charge transport with surprisingly large mobilities between 0.01 and 0.4 $cm^2/V{\cdot}s$. This high mobility is attributed to strong intermolecular interactions reinforcing π-stacking and crystalline ordering. This motivated us to look at a hydrogen-bonded analog of pentacene, quinacridone, with respect to charge transport in organic field-effect transistors (OFETs) and photogeneration in single-layer organic diodes. Quinacridone is a well-known commercial paint and cosmetic pigment.[6] It shows field-effect mobilities of 0.1 cm^2/Vs, photocurrents in the mA/cm^2 range under simulated solar illumination. Quinacridone thin films show an intrinsic charge generation mechanism that is unaffected by the presence of C_{60}.

Figure 1(a) shows the chemical structures of both pentacene and quinacridone. Pentacene is a five ring π-conjugated molecule, whereas in quinacridone, the intramolecular π-conjugation is broken. The optically determined band gaps of pentacene and quinacridone in solution and in films are shown in Fig. 1(b). Whereas the weak intermolecular van der Waals forces in pentacene cause only a slight decrease in the band gap and change in color, the amine and carbonyl groups in quinacridone participate in $=O\cdots H\text{-}N$ intermolecular hydrogen bonds with two neighboring molecules. In dilute solutions, quinacridone is pale yellow; only in the solid state, it adopts its characteristic red color, signaling the involvement of strong intermolecular interactions.[7,8]

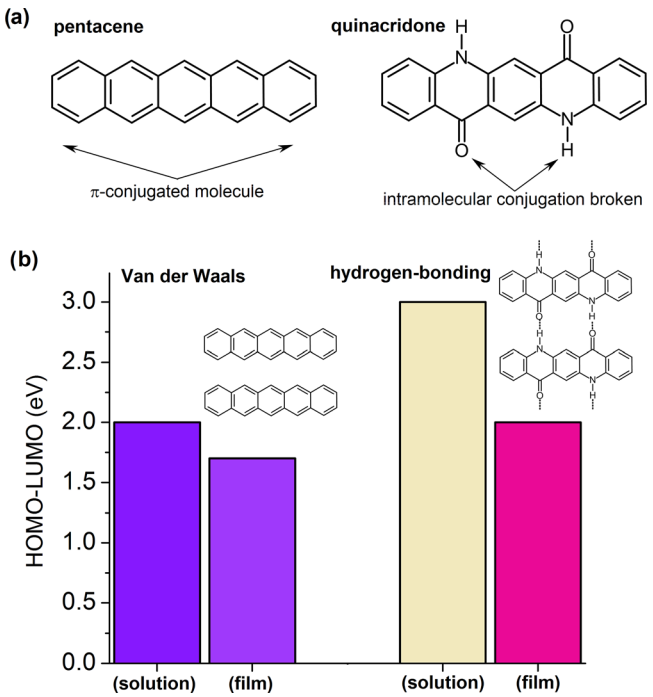

FIG. 1. (a) The molecular structures of pentacene and quinacridone. (b) The HOMO-LUMO band gap of pentacene and quinacridone, with the color of the bars representing the color of the molecules in dilute solutions and in solid state. The strong absorbance of green light resulting in red/violet colour of quinacridone occurs only in the solid state due to strong electronic coupling between neighboring molecules mediated by hydrogen bonding.

[a)]Author to whom correspondence should be addressed. Electronic mail: eric_daniel.glowacki@jku.at.

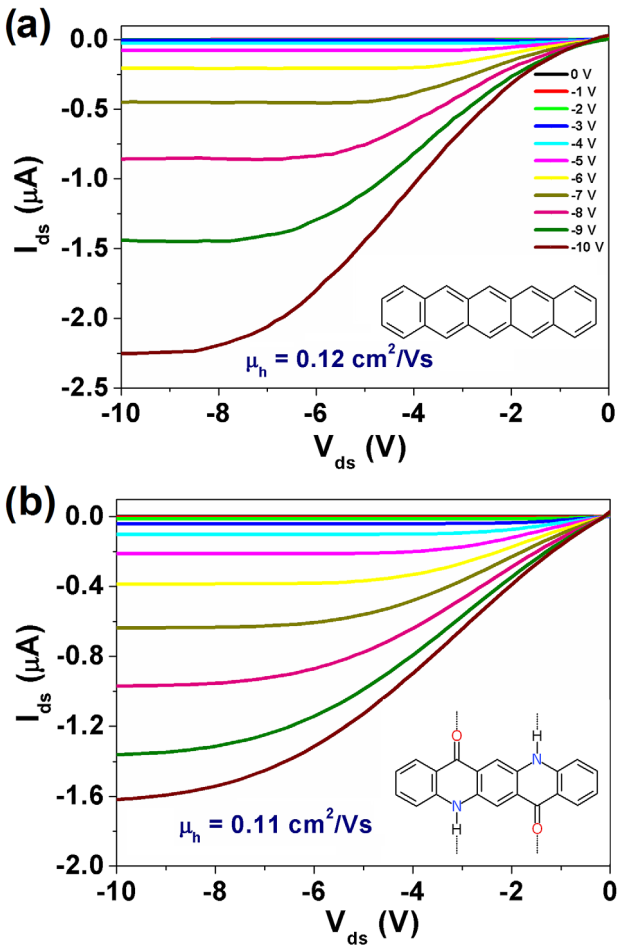

FIG. 2. OFET output characteristics for a pentacene device (a) and a quinacridone device (b).

For fabrication and measurement details of the devices, see supplementary material.[30] Highest-occupied molecular orbital (HOMO) and lowest-unoccupied molecular orbital (LUMO) levels of pentacene and quinacridone were estimated from cyclic voltammetry (CV),[9] with thin-films evaporated on indium tin oxide (ITO) functioning as the working electrode. CV data are shown in the supplementary material.[30] The dielectric constant (ε_r) was found from impedance measurements of metal-insulator-metal structures at sufficiently high frequencies (>0.1 MHz), and cross-checked by using different organic layer thicknesses and different metals. Mobility of quinacridone and pentacene was determined in OFET devices (supplementary material[30]). With a width W over length L ratio of W/L = 2 mm/75 μm, we obtained field-effect mobilities of 0.1 $cm^2/V{\cdot}s$ for holes. A comparison of output characteristics of quinacridone and pentacene transistors is shown in Figure 2. Pentacene devices with the same W/L ratio also show a hole mobility of ~0.1 $cm^2/V{\cdot}s$, consistent with earlier reports with similar device structures.[10] Further details on quinacridone in OFETs will be reported in a forthcoming publication. A comparison of the HOMO and LUMO levels, the band gap, and the field-effect charge mobilities of the two semiconductor molecules are shown in Table I. These results clearly show the competitive performance of quinacridone in OFETs. Its mass-availability, low cost, and stability[4] suggest it as an alternative to expensive and less-stable pentacene. Quinacridone crystallizes in the γ polymorph when sublimed, with a

TABLE I. Comparison of properties of pentacene and quinacridone. OFET devices with pentacene and quinacridone were prepared identically, using a W/L of 2 mm/75 μm. Pentacene mobility is consistent with previous reports for such channel geometries, see Ref. 10.

Material	HOMO (eV)	LUMO (eV)	E_g (CV)	E_g (optical)	ε_r	OFET μ_h ($cm^2/V{\cdot}s$)
Pentacene	−5.5	−3.3	2.2	1.7	3.9	0.1
Quinacridone	−5.4	−2.9	2.5	2	4.2	0.1

relatively tight π-stacking distance of 3.4 Å.[11,12] This packing is unlike the detrimental herringbone pattern in pentacene.[13] From x-ray diffraction of our thin films (supplementary material[30]), we see only the [002] peak in the growth direction, indicating a "standing-up" conformation of quinacridone molecules with π-stacking parallel to the substrate and thus favorable for charge transport in transistor geometry.

The promising charge transport properties of quinacridone motivated us to look at photogeneration in such hydrogen-bonded dyes in single-layer diodes. It is known that strong intermolecular interactions result in the dominance of excimeric effects dictating the optical properties of hydrogen-bonded dyes such as diketopyrrolopyrroles[14] and quinacridones.[8] Single-layer organic photovoltaic devices typically show poor performance because the high exciton binding energy in organic materials results in very low photocurrent densities not exceeding the $\mu A/cm^2$ range under solar illumination, corresponding to monochromatic quantum efficiencies of <1%. This obstacle was overcome in organic materials by using heterojunctions between electron-donor and electron-acceptor materials. The offset of molecular orbital energies of neighboring molecules allows efficient polarization of excitons generated by light absorption and photocurrent yields are enhanced by several orders of magnitude.[15,16] The donor-acceptor concept is at the heart of all organic solar cells at present, currently achieving efficiencies close to 10%.[17,18] However, the energetic offset between donor and acceptor results in a potential energy loss.[19,20] This decreases the photovoltage produced by such cells. Also, obtaining optimum nanomorphology between donor and acceptor domains is challenging and often demixing of the two components leads to stability problems in devices.[21]

In the performance of single-layer photovoltaic devices, quinacridone shows substantial advantage over pentacene. Figure 3 shows the J-V characteristics of pentacene and quinacridone metal-insulator-metal (MIM) diodes. Devices consisted of ITO coated with poly(3,4-ethylenedioxythiophene): poly(styrenesulfonate) (PEDOT:PSS) as the substrate, 100 nm of vacuum-evaporated organic semiconductor, and an evaporated aluminum top electrode. Quinacridone diodes show remarkable photocurrents in the mA/cm^2 range under 1.5 AM illumination, while pentacene produced only ~10 $\mu A/cm^2$. Quinacridone MIM devices showed open-circuit voltage (V_{oc}) scaling with the top contact metal work function (inset of Figure 3(b)) and fill factors of 30%–35%. These observations are consistent with reported organic MIM devices.[22] Importantly, the short circuit current was independent of metal work function. The external quantum efficiency (EQE) of quinacridone was between 1% and 10% over the range where the dye absorbs.

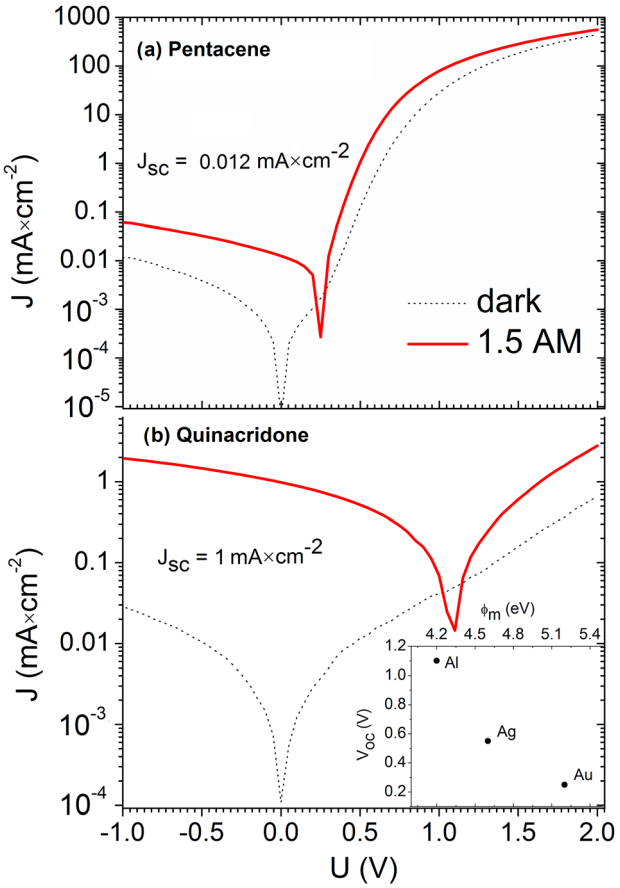

FIG. 3. Current-voltage (J-V) characteristics of ITO|PEDOT:PSS(40 nm)|semiconductor (100 nm)|Al (150 nm) diodes (a) pentacene, and (b) quinacridone in the dark and under simulated AM 1.5 illumination. The V_{oc} of quinacridone diodes with different top-contact metals is plotted versus metal work function in the inset of (b).

The EQE overlaid with the absorption coefficient for both dyes is plotted in Figure 4. We found that the external quantum efficiency of pentacene devices was 10^{-3} to 10^{-2}%. This is consistent with earlier reports of photogeneration in pentacene diodes.[23] These values are similar to single-layer devices with semiconducting polymers such as poly(phenylene vinylene)[24] and poly(thiophene),[25] where quantum efficiencies remain <1%. We conclude that the larger photocurrent yield of quinacridone versus pentacene is explained by the more efficient polarization of excitons into free carriers in quinacridone.

To interpret this phenomenon, we propose two explanations based on hydrogen bonding: (1) The larger strength of hydrogen bonds in intermolecular interactions relative to van der Waals bonds causes the high dielectric constant of quinacridone ($\varepsilon_r = 4.2$ vs. 3.9 in pentacene). A large dielectric coefficient ε_r leads to a lower exciton binding energy.[1] However, the difference between the estimated values of the exciton binding based on a dielectric constant difference of ~0.3 is not enough to account for the large discrepancy in the photogeneration of carriers. (2) Efficient formation of intermolecular charge transfer (CT) complexes that easily polarize into free-charges. We measured the photoluminescence of quinacridone films in comparison to quinacridone solutions (Figure 5). Relative to solutions, in films we found a 100–200 nm red-shifted and very broad emission peak suggesting the role of a CT state in dominating luminescence.

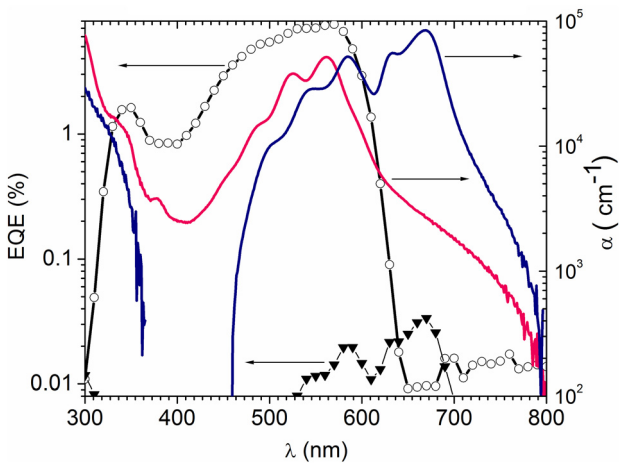

FIG. 4. External quantum efficiency (left axis) of ITO|PEDOT:PSS|semiconductor(100 nm)|Al diodes quinacridone (○, open circles) and pentacene (▼, filled triangles). Absorption coefficient (right axis) of evaporated thin films of quinacridone (pink) and pentacene (blue).

Time-resolved photoluminescence and electroabsorption studies reported by Kalinowski *et al.* showed that in the solid state of quinacridone, an initially formed singlet state self-traps into an excimeric CT state within 5 ps.[26,27] Optical studies of quinacridone in solution and solid state show that the transition dipole for the lowest-energy absorption aligns along the hydrogen bonding of neighboring molecules and that blocking the hydrogen bonding chemically will eliminate this absorption, supporting the idea of CT excitons delocalizing effectively between molecules due to hydrogen bonding.[8] To provide a preliminary estimate of the effective exciton binding energy in the quinacridone film, we measured the temperature dependence of photocurrent in a lateral geometry.[28] From the thermal activation of photocurrent, we estimate an exciton binding energy of ~12 ± 5 meV (supplementary material[30]). In an attempt to enhance photogeneration of carriers, C_{60}/quinacridone heterojunctions were

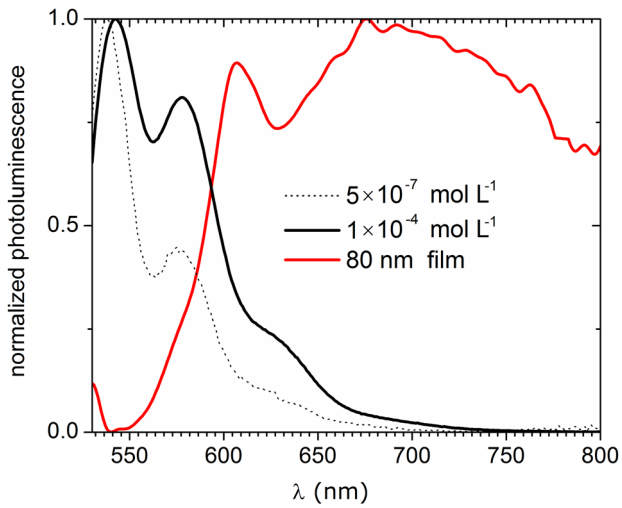

FIG. 5. (a) Room temperature photoluminescence of quinacridone in DMSO solutions and deposited as a thin-film on glass. The red-shifted and broad emission peak from quinacridone in the solid state is consistent with emission from dissociative states reported previously for hydrogen-bonded dyes, see Refs. 8, 12, 14, and 27.

prepared. Both pentacene and quinacridone, by virtue of the position of their respective HOMO and LUMO levels, should afford photoinduced charge transfer to C_{60}. The pentacene/C_{60} donor-acceptor system is well-characterized and shows electron transfer.[29] We found, in contrast, that the diodes with C_{60}/quinacridone showed no enhancement of photocurrent/EQE relative to quinacridone alone. This indicates that the mechanism responsible for generation of free charge carriers in quinacridone occurs faster than the photoinduced charge transfer to fullerene.

In conclusion, though lacking the intramolecular conjugation normally considered requisite for organic semiconductors, quinacridone in OFETs performs similarly to its analog pentacene. As such quinacridone presents itself as a stable and mass-available alternative to pentacene in organic electronics. Photogeneration in quinacridone occurs with at least a hundred times higher efficiency than in pentacene, an observation we attribute to excimeric effects known to occur in hydrogen-bonded organic dyes. Molecules with intermolecular hydrogen bonds have not been explored in organic photovoltaic applications; this preliminary research suggests this materials class for further exploration.

This work was partially funded by the Austrian Science Foundation "FWF" within the National Research Network NFN on Interface Controlled and Functionalized Organic Films (S09711-N08 and S09712-N08). Financial support from the city of Linz and the Land Oberösterreich is highly appreciated. Partial funding by the Sectoral Operational Programme Human Resources Development 2007-2013 of the Romanian Ministry of Labour, Family and Social Protection through the Financial Agreement POSDRU/88/1.5/S/60203 is gratefully acknowledged. The authors warmly thank Uwe Monkowius, Matthew White, Markus Scharber, and Toan Pho for fruitful discussions.

[1]M. Pope and C. E. Swenberg, *Electronic Processes in Organic Crystals and Polymers*, 2nd ed. (Oxford University Press, New York, 1999).
[2]A. Facchetti, Chem. Mater. **23**, 733 (2011).
[3]A. Pron and P. Rannou, Prog. Polym. Sci. **27**, 135 (2002).
[4]M. Irimia-Vladu, E. D. Głowacki, P. A. Troshin, G. Schwabegger, L. Leonat, D. K. Susarova, O. Krystal, M. Ullah, Y. Kanbur, M.-A. Bodea, V. F. Razumov, H. Sitter, S. Bauer, and N. S. Sariciftci, Adv. Mater. **24**, 375 (2012).
[5]E. D. Głowacki, L. Leonat, G. Voss, M.-A. Bodea, Z. Bozkurt, A. Montaigne Ramil, M. Irimia-Vladu, S. Bauer, and N. S. Sariciftci, AIP Adv. **1**, 042132 (2011).
[6]H. Zollinger, *Color Chemistry: Syntheses, Properties, and Applications of Organic Dyes and pigments*, 3rd ed. (Wiley-VCH, Weinheim, 2003).
[7]F. H. Chung and R. W. Scott, J. Appl. Cryst. **4**, 506 (1971).
[8]J. Mizuguchi and T. Senju, J. Phys. Chem. B **110**, 19154 (2006).
[9]C. M. Cardona, W. Li, A. E. Kaifer, D. Stockdale, and G. C. Bazan, Adv. Mater. **23**, 2367 (2011).
[10]C. S. Suchand Sangeeth, P. Stadler, S. Schaur, N. S. Sariciftci, and R. Menon, J. Appl. Phys. **108**, 113703 (2010).
[11]N. Nishimura, T. Senju, and J. Mizuguchi, Acta Crystallogr., Sect. E: Struct. Rep. Online **62**, 4683 (2006).
[12]E. F. Paulus, F. J. J. Leusen, and M. U. Schmidt, CrystEngComm. **9**, 131 (2007).
[13]R. C. Haddon, X. Chi, M. E. Itkis, J. E. Anthony, D. L. Eaton, T. Siegrist, C. C. Mattheus, and T. T. M. Palstra, J. Phys. Chem. B **106**, 8288 (2002).
[14]J. Mizuguchi, J. Phys. Chem. A. **104**, 1817 (2000).
[15]C. W. Tang, Appl. Phys. Lett. **48**, 183 (1986).
[16]N. S. Sariciftci, L. Smilowitz, A. J. Heeger, and F. Wudl, Science **258**, 1474 (1992).
[17]M. A. Green, K. Emery, Y. Hishikawa, W. Warta, and E. D. Dunlop, Prog. Photovoltaics **20**, 12 (2011).
[18]A. J. Heeger, N. S. Sariciftci, and E. B. Namadas, *Semiconducting and Metallic Polymers* (Oxford Graduate, USA, 2010).
[19]M. C. Scharber, D. Mühlbacher, M. Koppe, P. Denk, C. Waldauf, A. J. Heeger, and C. J. Brabec, Adv. Mater. **18**, 789 (2006).
[20]K. Vandewal, K. Tvingstedt, A. Gadisa, O. Inganäs, and J. V. Manca, Nature Mater. **8**, 904 (2009).
[21]M. Jørgensen, K. Norrman, and F. C. Krebs, Sol. Energy Mater. Sol. Cells **92**, 686 (2008).
[22]D. L. Morel, E. L. Stogryn, A. K. Ghosh, T. Feng, P. E. Purwin, R. F. Shaw, C. Fishman, G. R. Bird, and A. P. Piechowski, J. Phys. Chem. **88**, 923 (1984).
[23]C. Voz, J. Puigdollers, I. Martín, D. Muñoz, A. Orpella, M. Vetter, and R. Alcubilla, Sol. Energy Mater. Sol. Cells **87**, 567 (2005).
[24]R. N. Marks, J. J. M. Halls, D. D. C. Bradley, R. H. Friend, and A. B. Holmes, J. Phys.: Condens. Matter **6**, 1379 (1994).
[25]S. Glenis, G. Horowitz, G. Tourillon, and F. Garnier, Thin Solid Films **111**, 93 (1984).
[26]J. Kalinowski, W. Stampor, P. Di Marco, and V. Fattori, Chem. Phys. **182**, 341–352 (1994).
[27]L. Rossi, G. Bongiovanni, A. Borghesi, G. Lanzani, J. Kalinowski, A. Mura, and R. Tubino, Synth. Met. **84**, 873 (1997).
[28]G. Horowitz, P. Valat, P. Delannoy, and J. Roussel, Phys. Rev. B **59**, 651–656 (1999).
[29]S. Yoo, W. Potscavagejr, B. Domercq, S. Han, T. Li, S. Jones, R. Szoszkiewicz, D. Levi, E. Riedo, and S. Marder, Solid-State Electron. **51**, 1367 (2007).
[30]See supplementary material at http://dx.doi.org/10.1063/1.4736579 for device fabrication details, cyclic voltammetry data, impedance spectroscopy, X-ray diffraction data, and photocurrent vs. temperature measurements for exciton binding energy estimation.